Facultad de Ciencias Naturales y Exactas
Universidad del Valle

EFFECTS OF THE VIBRATIONAL MOTION OF XHY^- ON THE POST-PHOTO DETACHMENT DISSOCIATION DYNAMICS OF THE XHY COMPLEX (X, Y = Br, I)

Vivianne K. Ocampo-Restrepo **Julio C. Arce** **José G. López**
Universidad del Valle

Received: November 15, 2013 Accepted: December 23, 2013

Pág. 67-79

Abstract

We explore the effects of the transition-state vibrational motions on the dynamics of the reaction $X + HY \rightarrow [XHY]^{\ddagger} \rightarrow XH + Y$ with X and Y = Br, I. We performed simulations of the dissociation process of the unstable XHY complex using a classical trajectory methodology, combined with London-Eyring-Polanyi-Sato (LEPS) potentials to approximate the interactions among the atoms in XHY. We employed an almost classical sampling scheme on the stable XHY^- species to obtain the initial conditions for the trajectories by assuming a vertical transition to the XHY neutral potential energy surface. To study the effects of the vibrations, we considered different sets of initial conditions reflecting specific XHY normal mode excitations. We found an increase in the rotational energies of the product diatoms with an increase in the energy associated to the bending normal modes of XHY. Analysis of the vibrational distributions of the diatoms shows higher most probable vibrational quantum numbers for HBr when compared to HI. For some initial conditions, we also found approximately thermal rotational distributions in the product diatoms.

Keywords: Reaction dynamics, transition state, classical trajectories, electron photodetachment spectroscopy, vibrational normal modes, rotational states of molecules.

1 Introduction

The process of bond breaking and bond formation is of particular importance in the description of a chemical reaction. One way to study this process is through an unstable complex of short existence called the transition state [1]. Several experimental techniques have been developed to investigate how the transition state evolves. One of these techniques involves the preparation of a stable negative ion as a precursor. If the transition state of a neutral chemical reaction is similar in geometry to this ionic species, a fast detachment of the extra electron allows reaching the transition state region of the reaction of interest. Measurement of the kinetic energy, in the form of a photoelectron spectrum of the outgoing electron, provides information about the internal motion of the transition state [2].

Neumark and colleagues have applied anion photodetachment techniques for the study of bimolecular reaction of the type X + HY → XH + Y, where X and Y are halogen atoms [3, 4, 5, 6, 7, 8]. They observed a strong progression in the anti-symmetric stretch of the XHY neutral complex. They also observed more closely spaced progressions that reflects transitions to symmetric stretch and hindered rotor levels of XHY. Additionally, they investigated the effects of introducing solvating atoms and molecules on the transition state of these reactions [9, 10, 11].

Photo detachment of XHY^- ions have also been investigated using theoretical tools [12, 13, 14]. These studies have been fundamental in the assignment of the photoelectron spectra peaks to the different internal motions of the XHY complex [15]. They also have provided evidence of a caging effect caused by surrounding argon atoms in the dynamics of XHX [16, 17, 18].

In this paper, we report the results of a classical trajectory study of the dissociation dynamics of XHY complexes (X, Y = I, Br). Our interest is to investigate the effects of the vibrational motions of the XHY^- ionic species in the dissociation dynamics of XHY when it reaches the X + HY and Y + HX reaction channels. Specifically, we analyze how the initial vibrational energy of the XHY complex, assuming a vertical transition from the corresponding vibrating XHY^- ionic species, is redistributed into the rotational and vibrational motions of the resulting HX and HY diatoms and the translational motion of the resulting X and Y single atoms.

Although quantum effects are expected to be important, a classical methodology will provide us with physical insights into the dynamics of the system of interest in a way that is less computationally demanding than a quantum calculation. With this, we want to explore the use of appropriate approximate methodologies in the study of the dynamics of molecular systems, in particular the dynamics of chemical reactions at the molecular level.

2 Theory

2.1 Model potentials

The specification of the initial conditions will require the potential-energy surface (PES) of the XHY^- stable ionic system around the equilibrium configuration (Subsection 2.2). We approximate this potential as a multidimensional harmonic potential in normal mode coordinates [19]

$$V_{\mathrm{XHY}^-} = V_{\mathrm{eq}} + \sum_{k=1}^{4} \lambda_k Q_k^2 \tag{1}$$

where λ_k are the normal mode frequencies, Q_k is the kth normal mode coordinate and V_{eq} is the equilibrium potential energy. The values of λ_k for $BrHBr^-$ and $BrHI^-$ are given in Ref. [11] and for IHI^- in Ref. [15].

We used a London-Eyring-Polanyi-Sato (LEPS) potential [20] for XHY. Essentially, a LEPS potential is a semi-empirical potential based on the London equation for the H + H_2 system. Although, in general, this type of potential does not represent faithfully intra-molecular interactions [21], it should provide a reasonable interaction potential for our unstable neutral system. It takes the form:

$$V_{XHY} = \frac{Q_{XH}}{1+S_{XH}} + \frac{Q_{HY}}{1+S_{HY}} + \frac{Q_{XY}}{1+S_{XY}} - \left\{ \frac{1}{2}\left[\left(\frac{\alpha_{XH}}{1+S_{XH}} - \frac{\alpha_{HY}}{1+S_{HY}} \right)^2 + \left(\frac{\alpha_{HY}}{1+S_{HY}} - \frac{\alpha_{XY}}{1+S_{XY}} \right)^2 + \left(\frac{\alpha_{XY}}{1+S_{XY}} - \frac{\alpha_{XH}}{1+S_{XH}} \right)^2 \right] \right\}^{1/2} \quad (2)$$

Here, Q_{ij} and S_{ij} are obtained from a combination of Morse and anti-Morse potentials,

$$\frac{Q_{ij}+\alpha_{ij}}{1+S_{ij}} = D_{e,ij}\left[e^{-2\beta_{ij}(r_{ij}-r_{e,ij})} - 2e^{-\beta_{ij}(r_{ij}-r_{e,ij})} \right],$$
$$\frac{Q_{ij}-\alpha_{ij}}{1-S_{ij}} = D_{e,ij}\left[e^{-2\beta_{ij}(r_{ij}-r_{e,ij})} + 2e^{-\beta_{ij}(r_{ij}-r_{e,ij})} \right], \quad (3)$$

where r_{ij} is the distance between the *i*th and *j*th atoms, and $r_{e,ij}$, $D_{e,ij}$, and β_{ij} are parameters associated with a Morse potential for the isolated *i*-*j* diatom, which are adjusted by experimental data. The parameters for the LEPS potential for BrHBr are given in Ref. [5], for BrHI in Ref. [22], and for IHI in Ref. [23]. In figure 1 we plot the LEPS potentials for BrHBr and BrHI in their collinear configurations.

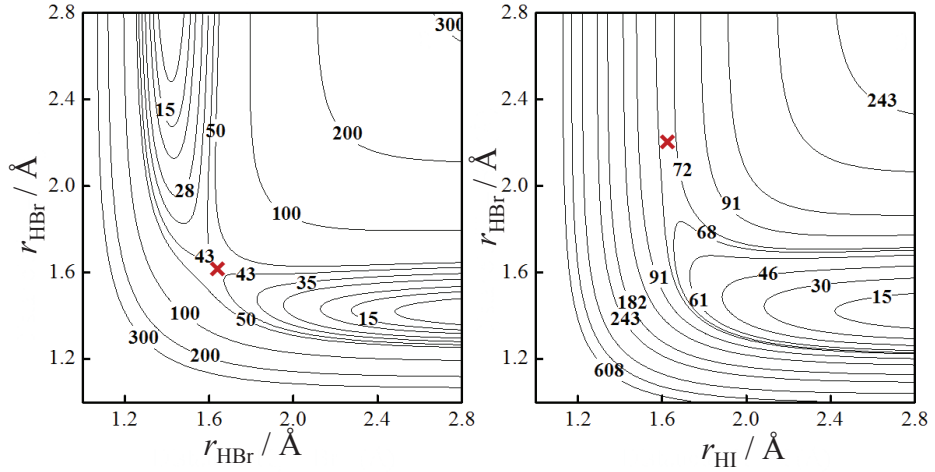

(a) *(b)*

Figure 1. *LEPS potential for the collinear configuration of (a) BrHBr and (b) BrHI. Energies are in kJ/mol. The red × symbol indicates the transition state.*

2. 2 Specification of initial conditions

The initial conditions for the integration of the classical equations of motion on the XHY PES (Subsection 2.3) were generated assuming a vertical transition from the XHY^- PES, i.e. a photodetachment of an electron in the Condon approximation.

A quasi-classical sampling of initial conditions [24] was performed in the four normal mode coordinates that describe the XHY^- vibrational motion. In this sampling, the energies of the vibrational normal modes are quantized but the phase-space probability distribution is that of a multidimensional classical harmonic oscillator. The normal coordinates are obtained by diagonalization of the matrix of second derivatives of the potential with respect to the mass-weighted Cartesian coordinates and evaluation at the minimum of the potential [19].

Once the initial conditions are obtained in normal mode coordinates, they are transformed into Cartesian coordinates by the diagonalizing matrix obtained from the diagonalization process described above [17].

2.3 Propagation

We propagated the dynamics of XHY by solving Newton's equations of motion for each set of initial positions and momenta of the X, H, and Y atoms in Cartesian coordinates,

$$\mathbf{F}_i = \frac{d\mathbf{p}_i}{dt} = m_i \frac{d^2\mathbf{x}_i}{dt^2}, \quad (i = \mathrm{X,H,Y}) \tag{4}$$

employing the Gear algorithm [25] with time steps ranging from 0.1 a.u. to 2 a.u. The wall computer processing time for a single trajectory integrated for 7 ps was 0.25 seconds on a 3.47 GHz Six Core Intel-Xeon processor with 12 GB RAM.

3 Results and discussion

3.1 Initial conditions

To investigate how the initial vibrational motion of XHY affects the vibrations and rotations of the product HX or HY diatoms, we used different sets of initial conditions in normal-mode coordinates. In figure 2 we illustrate the normal modes of the XHX^- system. We employed the following notation: $Q_k(n)$ means that there are n quanta of excitation in the k-th normal mode, with k=s,a,b_1,b_2 representing the symmetric, anti-symmetric, and two degenerate bending modes. Thus, $Q(0) \equiv [Q_s(0), Q_a(0), Q_{b1}(0), Q_{b2}(0)]$ represents the vibrational ground state, $Qs(n) \equiv [Q_s(n), Q_a(0), Q_{b1}(0), Q_{b2}(0)]$ represents a state

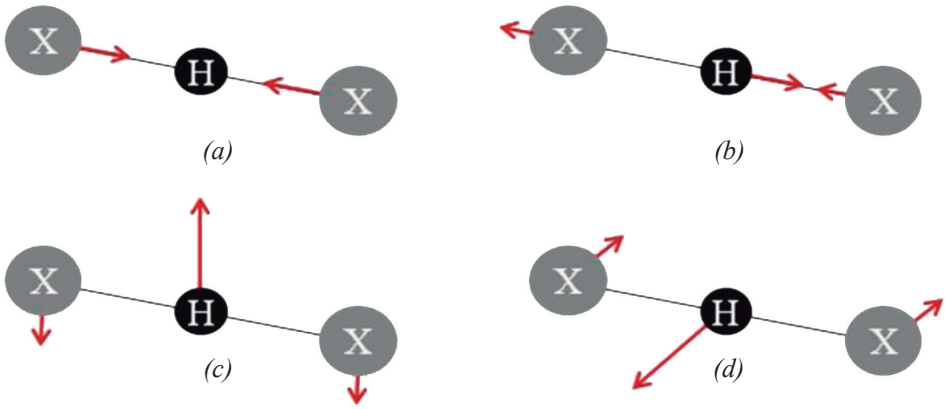

Figure 2. *Vibrational normal modes for XHY^-. (a) Symmetric normal mode, Q_s. (b) Anti-symmetric normal mode, Q_a. (c) Bending normal mode, Q_{b1}. (d) Bending normal mode, Q_{b2}.*

With n quanta in the symmetric mode, $Qa(n) \equiv [Q_s(0), Q_a(n), Q_{b1}(0), Q_{b2}(0)]$ represents a state with n excitations in the asymmetric mode, $Qb(n) \equiv [Q_s(0), Q_a(0), Q_{b1}(n), Q_{b2}(0)]$ represents a state with n excitations in one of the bending modes, and $Qb(n,n) \equiv [Q_s(0), Q_a(0), Q_{b1}(n), Q_{b2}(n)]$ represents a state with n simultaneous excitations of the two degenerate bending modes. We considered only excitations with $n = 1, 2$.

After fixing the sets of normal-mode quantum numbers, we employed the method described in Section 2.2 to obtain the corresponding initial conditions in Cartesian coordinates for each set.

3.2 Product channels

We propagated 10 000 trajectories for each set of initial conditions described above. In table 1 we present the percentage of trajectories evolving into the two reaction channels (HX + X and X + HX) for each system, as a function of the initial conditions.

Table 1. *Percentage of trajectories for the different reaction channels as functions of the different initial condition sets described in Section 3.*

	IHI		BrHBr		BrHI	
	IH + I	I + HI	BrH + Br	Br + HBr	BrH + I	Br + HI
$Q(0)$	50.2	49.8	50.7	49.3	59.9	40.1
$Qs(1)$	50.0	50.0	50.7	49.3	61.3	38.7
$Qs(2)$	49.9	50.1	50.8	49.2	60.7	39.3
$Qa(1)$	50.0	50.0	50.8	49.2	57.5	42.5
$Qa(2)$	50.7	49.3	50.8	49.2	70.0	30.0
$Qb(1)$	50.2	49.8	50.9	49.1	60.0	40.0
$Qb(2)$	50.3	49.7	50.7	49.3	61.3	38.7
$Qb(1,1)$	50.6	49.4	50.6	49.4	60.6	39.4
$Qb(2,2)$	50.1	49.9	50.7	49.3	61.1	38.9

For IHI and BrHBr we found that each channel comprises approximately half of the trajectories, for all sets of initial conditions. This is an expected result given the symmetry of the PES (figure 1(*a*)). On the other hand, for BrHI we found that the major reaction channel is I + HBr, a result surely associated with the asymmetric shape of the PES (figure 1(*b*)).

To explain the observed 20% differences in the number of trajectories of the latter case, it is necessary to take into account *potential* and *kinetic* energy factors. Specifically, in the minimum-energy path for the reaction Br + HI → $[BrHI]^{\#}$ → I + HBr, the I + HBr and Br + HI channels have energy barriers of 70.75 $kJmol^{-1}$ and 0.87 $kJmol^{-1}$, respectively, in the collinear configuration, and at any bent configuration these barriers increase by equal amounts. Moreover, the transition state is much closer to the Br + HI channel than to the I + HBr one. On grounds of these asymmetries, it is expected that the number of trajectories entering the Br + HI channel and bouncing into the I + HBr channel to be much greater than the number of trajectories that entering the I + HBr channel and bouncing into the Br + HI channel. However, since in the transition-state configuration the I–H distance is much smaller than the H–Br distance, then the initial distributions of positions and momenta for BrHI are biased for the Br + HI channel, contributing, therefore to an increase in the number of trajectories entering this channel. The balance between these two kinds of effects explains why the difference in the percentages are not large.

3.3 Energy redistribution in the products

When the XHY complex breaks apart, its energy is distributed among the different degrees of freedom of the resulting diatom and single atom. To analyze the energy partitioning, it is convenient to separate the motion of the single atom from the motion of the diatom by transforming the Hamiltonian from Cartesian into Jacobi coordinates [26]:

$$H = \frac{\mathbf{p}_{\mathrm{X}}^2}{2m_{\mathrm{X}}} + \frac{\mathbf{p}_{\mathrm{H}}^2}{2m_{\mathrm{H}}} + \frac{\mathbf{p}_{\mathrm{Y}}^2}{2m_{\mathrm{Y}}} + V(x_{\mathrm{X}}, y_{\mathrm{X}}, z_{\mathrm{X}}, x_{\mathrm{H}}, y_{\mathrm{H}}, z_{\mathrm{H}}, x_{\mathrm{Y}}, y_{\mathrm{Y}}, z_{\mathrm{Y}})$$

$$\downarrow$$

$$H = \frac{\mathbf{p}_{\mathbf{r}}^2}{2\mu_r} + \frac{\mathbf{P}_{\mathbf{R}}^2}{2\mu_R} + \frac{\mathbf{P}_{\mathrm{COM}}^2}{2M} + V(\mathbf{r}, \mathbf{R}) \tag{5}$$

For example, in the case XHY → X + HY, **r** is the vector between the two atoms in HY and **R** is the vector between the X atom and the center of mass (COM) of HY, $\mathbf{p}_{\mathbf{r}}$ and $\mathbf{P}_{\mathbf{R}}$ are the corresponding conjugate momenta, and μ_r and μ_R are the reduced masses of HY and X–HY, respectively. $\mathbf{P}_{\mathrm{COM}}$ is the COM momentum of XHY and M is the total mass of the system ($M = m_{\mathrm{X}} + m_{\mathrm{H}} + m_{\mathrm{Y}}$). If $\mathbf{P}_{\mathrm{COM}}$ is zero, then $\mathbf{p}_{\mathrm{X}} = \mathbf{P}_{\mathbf{R}}$ and the kinetic energy of the single atom reads

$$T_{\mathrm{X}} = \frac{\mathbf{p}_{\mathrm{X}}^2}{2m_{\mathrm{X}}} = \frac{\mathbf{P}_{\mathbf{R}}^2}{2m_{\mathrm{X}}} \tag{6}$$

Since asymptotically $V(\mathbf{r}, \mathbf{R}) = V(r)$, the total energy of the system becomes

$$E = \frac{\mathbf{p}_{\mathbf{r}}^2}{2\mu_r} + \frac{\mathbf{P}_{\mathbf{R}}^2}{2\mu_R} + V(r) \tag{7}$$

Therefore, the internal kinetic energy of the diatom is given by

$$T_{HY} = \frac{\mathbf{p}_r^2}{2\mu_r} = E - \frac{\mathbf{P}_R^2}{2\mu_R} - V(r) \tag{8}$$

which can be written as [27]

$$T_{HY} = \frac{1}{2}\mu_{HY}\dot{r}^2 + \frac{l^2}{2\mu_{HY}r^2} \tag{9}$$

where r is the magnitude of the vector $\mathbf{r}$, $\dot{r}$ is the time derivative of r, and l is the rotational angular momentum of HY. Therefore, the internal kinetic energy of the diatom can be separated into two contributions: the vibrational $\mu_{HY}\dot{r}^2/2$ and the rotational $l^2/(2\mu_{HY}r^2)$.

In figure 3 we show the energy redistribution of IHI into HI internal energy and I translational energy. These results show that a major portion of the energy is redistributed as vibrational energy of the diatom HI while little of it becomes kinetic energy of the single atom I. We also observe an increase of the rotational energy of HI when the IHI complex has initial excitations in the bending normal modes. This is due to the fact that an increase in the amplitude of the bending motion of IHI increases the velocity component of the H atom perpendicular to the I–I axis, which, in turn, increases the angular speed of the separating HI diatom. This behavior is also observed in BrHBr and BrHI. Table 2 lists the results of the energy redistribution of BrHBr into HBr internal energy and Br translational energy.

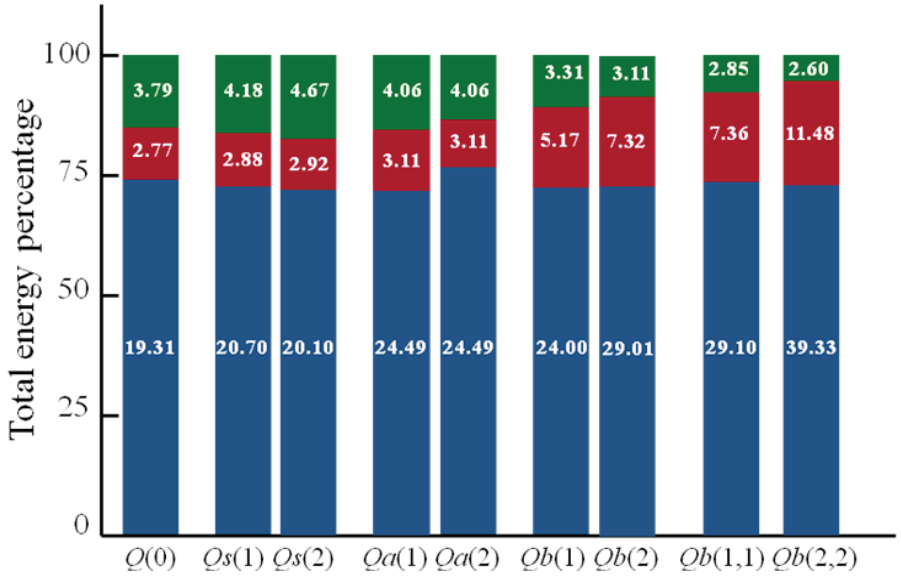

Figure 3. *Total energy redistribution percentage from IHI into HI internal energy and I translational energy as a function of the initial conditions (see subsection 3.3). The blue rectangle is the vibrational energy of HI, the red rectangle is the rotational energy of HI, and the green rectangle is the translational energy of the single atom I. The white numbers indicate the average energy, in kJ/mol, for each degree of freedom.*

Table 2. *Energy redistribution of BrHBr into HBr internal energy and Br translational energy. Energies are in kJ/mol. The numbers in parentheses give one standard deviation for the energy values.*

	Total energy	HBr		Br
		Vibrational energy	Rotational energy	Translacional energy
Q(0)	123.0 (0.2)	102.5 (0.2)	6.12 (0.07)	14.35 (0.02)
Qs(1)	123.6 (0.2)	102.6 (0.2)	6.19 (0.07)	14.85 (0.02)
Qs(2)	124.2 (0.2)	102.6 (0.2)	6.21 (0.07)	15.38 (0.03)
Qa(1)	98.8 (0.3)	78.0 (0.4)	6.40 (0.07)	14.39 (0.02)
Qa(2)	85.0 (0.4)	64.2 (0.5)	6.36 (0.07)	14.4 (0.02)
Qb(1)	132.1 (0.2)	108.3 (0.2)	9.6 (0.1)	14.25 (0.02)
Qb(2)	140.6 (0.2)	113.9 (0.2)	12.5 (0.2)	14.22 (0.02)
Qb(1,1)	141.3 (0.2)	114.2 (0.2)	13.0 (0.2)	14.20 (0.02)
Qb(2,2)	158.3 (0.2)	125.5 (0.3)	18.7 (0.2)	14.13 (0.02)

3.4 Vibrational and rotational populations of the product diatoms

There is no rigorous way to determine quantum vibrational states of the product diatoms from quasi-classical trajectory calculations. Here, we assign the vibrational quantum number *n* to a diatom if its energy is closest to the one of the *n*-th state of the corresponding quantum oscillator [28]. For the case of a LEPS potential, the asymptotic vibrational quantum states of the diatom are the ones of a Morse potential [27] whose eigenenergies are given by

$$E(n) = \left(n + \frac{1}{2}\right) h\nu_e - \left(n + \frac{1}{2}\right)^2 h\nu_e x_e; \quad n = 0,1,2,... \tag{10}$$

where ν_e and x_e are the harmonic frequency and the Morse anharmonicity term, respectively.

The rotational quantum number *j* for the diatom is found from:

$$l = \sqrt{j(j+1)}\hbar \tag{11}$$

where the angular momentum *l* is determined by:

$$l = \mu_{HY} \mathbf{r} \times \dot{\mathbf{r}} \tag{12}$$

Since this gives non-integer values for *j*, we rounded up the value of *j* to the nearest integer.

In table 3, we list the vibrational-state populations of the product diatoms as functions of the initial conditions for IHI and BrHBr. We found that for IHI the most probable vibrational state of the product diatom is $n = 0$, except when the bending modes of the parent complex are twice or four times excited, where the $n = 1$ population becomes dominant. For BrHBr we found a much broader distribution of the product diatom vibrational states, with $n = 3$ being the most probable state for most of the initial conditions. A comparison of the total energies of these two symmetric systems (see figure 3 and table 2 for the energy results of IHI and BrHBr, respectively) reveals that BrHBr contains more energy. That is why this complex exhibits a wider energy redistribution in all the product degrees of freedom. For BrHI (not shown), the vibrational distributions in the product diatoms HBr and HI exhibit similar behaviors as for BrHBr and IHI, respectively.

Table 3. *Percentage of trajectories, as functions of the initial conditions, in each vibrational quantum state of the product diatom from IHI and BrHBr.*

	HI			HBr						
	$n = 0$	$n = 1$	$n = 2$	$n = 0$	$n = 1$	$n = 2$	$n = 3$	$n = 4$	$n = 5$	$n = 6$
$Q(0)$	76.7	23.3				27.4	48.3	24.3		
$Qs(1)$	75.3	24.7				27.7	47.2	25.2		
$Qs(2)$	72.1	27.8			0.5	27.7	46.6	25.3		
$Qa(1)$	76.1	23.8		7.19	29.7	24.7	17.6	30.8		
$Qa(2)$	63.4	36.6		36.1	15.5	16.0	11.8	15.4	5.2	
$Qb(1)$	59.4	40.6				17.7	48.3	34.0		
$Qb(2)$	40.8	59.1			0.2	14.7	40.7	33.5	10.9	
$Qb(1,1)$	40.6	59.4			0.2	14.6	40.4	33.3	11.5	
$Qb(2,2)$	24.3	52.4	23.3		0.7	10.4	22.6	37.2	25.3	3.7

In figure 4, we display the rotational distributions of HI resulting from IHI dissociation. We observed that for some initial conditions the distributions look approximately thermal (Boltzmann-like). Similar results were found for the BrHBr and BrHI complexes (not shown). Considering that the distributions of initial conditions for the trajectories were obtained from fixed quantum vibrational states, this result is not obvious. Clearly, it must be related to the small spacing between the rotational energy levels in comparison with the total energy transferred to the diatom. This observation warrants a more detailed analysis, which will be undertaken elsewhere.

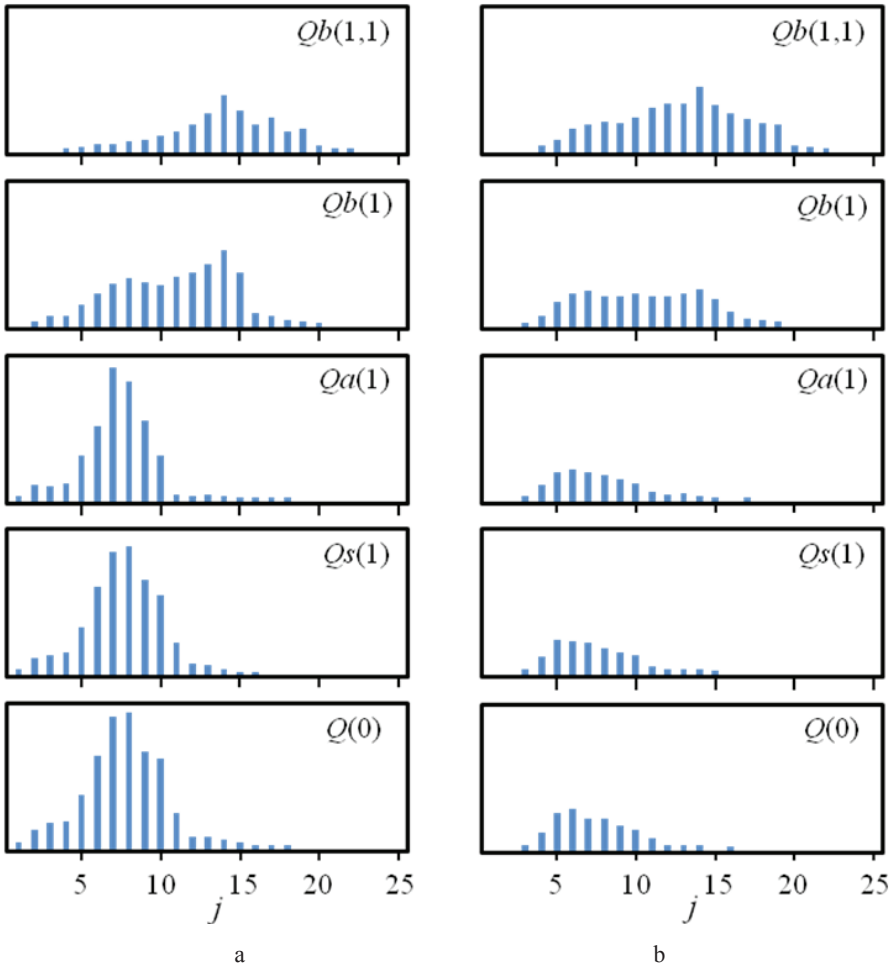

Figure 4. *Distribution of rotational states for the HI diatom, resulting from the dissociation of IHI, for (a) the vibrational quantum number n = 0 and (b) the vibrational quantum number n = 1. j is the rotational quantum number of HI.*

4 Summary and conclusions

We investigated the effects of the vibrational motions of the unstable complex XHY (X, Y = Br, I), resulting from a vertical transition of the corresponding stable XHY^- ionic species, on the vibrational and rotational motions of the product HX and HY diatoms. We used a classical trajectory method to evaluate the dynamics of the system with different sets of initial conditions that reflect specific XHY^- normal mode excitations.

The results show considerable effects of the initial vibrational states of XHY in the vibrational and rotational states of HX and HY. Specifically, we found an enhancement of the rotational motion of the diatoms when the bending normal modes of XHY were excited. For BrHI we found the I + HBr reaction product channel as the most probable

one, mainly due to the geometry of the transition state of the reaction Br + HI → $[BrHI]^‡$ → BrH + I, which is closer to the I + HBr channel. One interesting result that we found was a quasi-thermalized rotational distribution in the product diatoms, even though the initial vibrational normal mode distribution of XHY is not thermalized.

Although the results reported in this paper were obtained from classical- mechanical methodologies, they give us physical insight on how the total energy available to XHY gets partitioned in the different degrees of freedom of the products and the branching ratios of the different reaction product channels. This information will be useful for the design of strategies that will allow us to control the reaction product channel of the dissociating XHY complex and the final vibrational and rotational states of the product diatoms.

Acknowledgment

Financial support for this work was provided by Universidad del Valle.

Bibliography

[1] J. C. Polanyi y A. H. Zewail, Direct Observation of the Transition State, *Acc. Chem. Res.,* vol. 28, p. 119, 1995.

[2] D. M. Neumark, Transition-state spectroscopy via negative ion photodetachement, *Acc. chem. Res.,* vol. 26, p. 33, 1993.

[3] A. Weaver, R. B. Metz, S. E. Bradforth y D. M. Neumark, Spectroscopy of the I + HI Transition-State Region by Photodetachment IHI-, *J. Chem. Phys.,* vol. 92, p. 5558, 1988.

[4] R. B. Metz, T. Kitsopoulos, A. Weaver and D. M. Neumark, Study of the transition state region in the Cl + HCl resction by photoelectron spectroscopy of ClHCl-, *J. Chem. Phys.,* vol. 88, p. 1463, 1988.

[5] R. B. Metz, A. Weaver, S. E. Bradforth, T. N. Kitsopoulos y D. M. Neumark, Probing the transition state with negative ion photodetachment: the chlorine atom+ hydrogen chloride and bromine atom+ hydrogen bromide reactions, *J. Phys. Chem.,* vol. 94, p. 1377, 1990.

[6] D. M. Neumark, Transition state spectroscopy of bimolecular chemical reactions, *Rev. Phys. Chem.,* vol. 43, p. 153, 1992.

[7] S. E. Bradforth, A. Weaver, D. W. Arnold, R. B. Metz y D. M. Neumark, Examination of the Br + HI, and F + HI hydrogen abstraction reactions by photoelectron spectroscopy of BrHI-, ClHI-, and FHI-, *J. Chem. Phys. ,* vol. 92, p. 7205, 1990.

[8] R. B. Metz, S. E. Bradforth y D. M. Neumark, Transition state spectroscopy of bimolecular reactions using negative ion photodetachment, *Adv. Chem. Phys.,* vol. 91, p. 1, 1991.

[9] L. Zhuan, H. Gómez y D. M. Neumark, Photoelectron spectroscopy of clustered transition state precursors IHI- . Ar and BrHI-.Ar, *Chem. Phys. Lett. ,* vol. 332, p. 65, 2000.

[10] L. Zhuan, H. Gómez y N. D. M., Transition state spectroscopy of the I+ HI reaction in clusters: Photoelectron spectroscopy of IHI−· Arn (n= 1–15)., *Faraday Discussions,* vol. 118, p. 221, 2001.

[11] H. Gómez, G. Meloni, J. Madrid y D. M. Neumark, Anion photoelectron spectroscopy of solvated transition state precursors, *J. Chem. Phys. ,* vol. 119, p. 872, 2003.

[12] G. C. Schatz, A three dimensional reactive scattering study of the photodetachment spectrum of ClHCl−, *J. Chem. Phys.,* vol. 90, p. 3582, 1989.

[13] J. M. Bowman y B. Gazdy, A reduced dimensional L2 simulation of the photodetachment spectra of ClHCl- and IHI-, *J. Phys. Chem.,* vol. 93, p. 5129, 1989.

[14] K. Yamashita y K. Morokuma, Ab initio study of transition state spectroscopy: ClHCl− photodetachment spectrum, *J. Chem. Phys.,* vol. 93, p. 3716, 1990.

[15] R. B. Metz y D. M. Neumark, Adiabatic three-dimensional simulations of the IHI−, BrHI−, and BrHBr− photoelectron spectra, *J. Chem. Phys.,* vol. 97, p. 962, 1992.

[16] H. B. Lavender y A. B. McCoy, Transition state dynamics of Arn(ClHCl) (n=0-5): effects of complex formation on the dynamics and spectroscopy, *J. Phys. Chem. A,* vol. 104, p. 644, 2000.

[17] J. G. López y A. B. McCoy, Transition state dynamics of Ar(n).(IHI) (n = 0-20), *J. Phys. Chem. A ,* vol. 109, p. 1272, 2005.

[18] J. G. López y M. A. B., Photoelectron spectra of Arn(IHI)- (n = 0-6,12,20), a theoretical Study, *J. Phys. Chem. A,* vol. 110, p. 5450, 2006.

[19] I. Levine, Molecular spectroscopy, New York: John Wiley & Sons, Inc., 1975.

[20] S. Sato, On a new method of drawing the potential energy surface, *J. Chem. Phys.,* vol. 23, p. 592, 1955.

[21] J. I. F. J. S. Steinfeld y W. L. Hase, Chemical Kinetics and Dyamics 2 ed., Upper Saddle River: Prentice-Hall, Inc., 1999.

[22] M. Broida y A. Persky, Dynamics of the reactions Cl + HBr and Br + HI, *Chem. Phys.,* vol. 133, p. 405, 1989.

[23] I. Manz y J. Romelt, On the collinear I + HI and I + MuI reactions, *Chem. Phys. Lett.,* vol. 81, p. 179, 1981.

[24] L. M. Raff y T. D. L, The classical trajectory approach to reactive scattering, in *Theory of Chemical Reaction Dynamics Vol. 3*, Boca Raton, CRC Press, 1985, p. 1.

[25] M. P. Allen y D. J. Tildesley, Computer simulations of liquids, New York: Oxford University Press, 1989.

[26] N. E. Henriksen y H. F. Y., Theories of molecular reaction dynamics: the microscopic foundation of chemical kinetics, New York: Oxford University Press, 2008.

[27] W. L. Hase, Classical trajectory simulations: final conditions, in *Encyclopedia of Computational Chemistry*, New York, John Wiley & Sons, Ltd., 1998, p. 400.

[28] J. G. López y A. B. McCoy, Classical treatments of quantum mechanical effects in collisions of weakly bound complexes, *Chem. Phys.,* vol. 308, p. 267, 2005.

Author's address

Vivianne K. Ocampo-Restrepo
Departamento de Química, Universidad del Valle, Cali – Colombia
vivianne.ocampo@correounivalle.edu.co

Julio C. Arce
Departamento de Química, Universidad del Valle, Cali – Colombia
julio.arce@correounivalle.edu.co

José G. López
Departamento de Química, Universidad del Valle, Cali – Colombia
jose.g.lopez@correounivalle.edu.co